

Peripheral, ultrarelativistic production of particles in heavy ion collisions *

ANTONI SZCZUREK

Institute of Nuclear Physics PAN, PL-31-342 Cracow, Poland and
University of Rzeszów, PL-35-959 Rzeszów, Poland

The cross sections for the production of two-pions in ultraperipheral ultrarelativistic heavy ion collisions, calculated in the impact parameter Equivalent Photon Approximation (EPA), are presented. Differential distributions in impact parameter, dipion invariant mass, single pion and dipion rapidity, pion transverse momentum and pion pseudorapidity are shown. The $\gamma\gamma \rightarrow \pi^+\pi^-$ subprocess constitutes a background to the $AA \rightarrow A\rho^0(\rightarrow \pi^+\pi^-)A$ process, initiated by emission of a photon by one of colliding nuclei. Only a part of the dipion invariant mass distribution associated with the $\gamma\gamma$ -collisions can be visible as the cross section for the $AA \rightarrow A\rho^0A$ reaction is very large.

Differential distributions for two ρ^0 meson production in exclusive ultraperipheral, ultrarelativistic collisions via a double scattering mechanism are presented. The cross section for $\gamma A \rightarrow \rho^0 A$ is parametrized based on a calculation from the literature. Smearing of ρ^0 masses is taken into account. The results of calculations are compared to experimental data obtained at RHIC and to the contribution of the two-photon mechanism.

The double scattering mechanism populates larger $\rho^0\rho^0$ invariant masses and larger rapidity distances between the two ρ^0 mesons compared to the $\gamma\gamma$ fusion. It gives a significant contribution to the $AA \rightarrow AA\pi^+\pi^-\pi^+\pi^-$ reaction. Some observables related to charged pions are presented. The results of our calculation are compared with the STAR collaboration results for four charged pion production. While the shape in invariant mass of the four-pion system is very similar to the measured one, the predicted cross section constitutes only 20 % of the measured one.

PACS numbers: 25.75.Dw, 13.25.-k

* Presented at the XX Cracow EPIPHANY Conference on the Physics at the LHC

1. Introduction

Ultrarelativistic ultraperipheral production of mesons and elementary particles is a special class of nuclear reactions [1]. The ultrarelativistic heavy ions provide large fluxes of quasi-real photons. The photon emitted by one nucleus can collide with the other nucleus or another photon emitted by the second nucleus leading to different interesting final states. Both total photon-photon cross sections as well as cross section for particular simple final states are interesting. The nuclear cross section is often calculated in the Equivalent Photon Approximation in momentum space [2, 3]. Alternatively one uses impact parameter space approach [4, 3]. The impact parameter space is very convenient to exclude cases when both heavy ions collide with each other, i.e., when they do not survive the high-energy collision. In the momentum space calculation (EPA or full calculation) the effects of nucleus-nucleus collisions and their associated break-up are neglected. This effect is very small for light particle production such as e^+e^- but increases when the mass of the produced system becomes large.

In our past publications we have shown there the inclusion of realistic charge form factors, being Fourier transforms of realistic charge distributions, is essential for precise estimate of the nuclear cross sections.

In this presentation, we present results obtained within the impact parameter EPA for the exclusive production of $\pi^+\pi^-$ and $\pi^0\pi^0$. For $\rho^0\rho^0$ production till recently only the photon-photon mechanism was discussed in the literature [5, 6, 7, 9]. In Ref. [9] we have made a first realistic estimate of the corresponding cross section.

In this mini review we discuss also exclusive production of two ρ^0 mesons. The cross section for single ρ^0 meson production was predicted in the literature to be large [8, 19, 11]. Measurements performed at RHIC confirmed the size of the cross section [12], but were not able to distinguish between different models that predicted different behaviour on (pseudo)rapidity. The large cross section for single ρ^0 production means that the cross section for double scattering process is also large. The best example of a similar type of reaction is the production of $c\bar{c}c\bar{c}$ final state in proton-proton collisions which was measured recently by the LHCb collaboration [13]. In our studies [14] we predicted and explained the main trends of the data as a double-parton scattering effect. There, the cross section for the $c\bar{c}c\bar{c}$ final state is of the same order of magnitude as the cross section for single $c\bar{c}$ pair production. The situation for exclusive ρ^0 production is similar. Due to good control of absorption effect, the impact parameter formulation seems in the latter case to be the best approach.

In Ref.[18] we have studied differential single particle distributions for the ρ^0 mesons, as well as correlations between the ρ mesons, also for the

photon-photon component where also a comparison to the results for photon-photon process was done, in order to understand how to identify the double photoproduction process. In this analysis we have take into account the decay of ρ^0 mesons into charged pions, in order to take into account some experimental cuts of existing experiments. We shall discuss here how to identify the double-scattering mechanism at the LHC.

2. Formalism

In this section we sketch the formalism necessary to understand exclusive production of $\pi^+\pi^-$, $\pi^0\pi^0$, $\rho^0\rho^0$ and $\pi^+\pi^-\pi^+\pi^-$.

2.1. $\gamma\gamma \rightarrow \pi^+\pi^-$ and $\gamma\gamma \rightarrow \pi^0\pi^0$ processes

In Ref.[15] we have made a careful analysis of reaction mechanisms necessary to understand the situation for “elementary” processes $\gamma\gamma \rightarrow \pi^+\pi^-$ and $\gamma\gamma \rightarrow \pi^0\pi^0$. Here we shall not repeat details of that study. Instead in Fig.1 we show how we described corresponding world data for these processes.

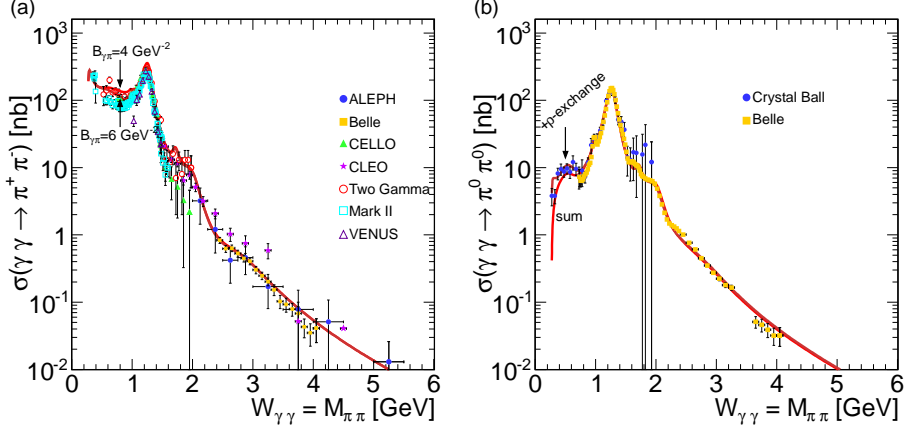


Fig. 1. (Color online) The total cross section for $\gamma\gamma \rightarrow \pi^+\pi^-$ (left panel, $|\cos\theta| < 0.6$) and $\gamma\gamma \rightarrow \pi^0\pi^0$ (right panel, $|\cos\theta| < 0.8$).

As discussed in the next section the elementary cross sections for $\gamma\gamma \rightarrow \pi\pi$ are building blocks for calculating corresponding cross sections for nuclear collisions. In the following we shall concentrate exclusively on the nuclear collisions.

2.2. Equivalent photon approximation for $AA \rightarrow AA\pi\pi$

The total nuclear cross section for these processes can be expressed by folding the $\gamma\gamma \rightarrow \pi\pi$ subprocess cross sections with equivalent photon fluxes as:

$$\sigma(AA \rightarrow AA\pi\pi; s_{AA}) = \int \hat{\sigma}(\gamma\gamma \rightarrow \pi\pi; W_{\gamma\gamma}) S_{abs}^2(\mathbf{b}) \times N(\omega_1, \mathbf{b}_1) N(\omega_2, \mathbf{b}_2) d^2\mathbf{b}_1 d^2\mathbf{b}_2 d\omega_1 d\omega_2. \quad (1)$$

At intermediate energies the Glauber approach is a reasonable approach to calculate the absorption factor $S_{abs}(\mathbf{b})$. Here we approximate the absorption factor as:

$$S_{abs}^2(\mathbf{b}) = \theta(\mathbf{b} - 2R_A) = \theta(|\mathbf{b}_1 - \mathbf{b}_2| - 2R_A). \quad (2)$$

This form excludes the geometrical configurations when the colliding nuclei overlap which at high energies leads to their breakup.

In order to simplify our calculation we use the transformations:

$$\omega_{1/2} = \frac{W_{\gamma\gamma}}{2} e^{\pm Y_{\pi\pi}}, \quad d\omega_1 d\omega_2 = \frac{W_{\gamma\gamma}}{2} dW_{\gamma\gamma} dY_{\pi\pi}. \quad (3)$$

The formula (1) can be written now as:

$$\sigma(AA \rightarrow AA\pi\pi; s_{AA}) = \int \hat{\sigma}(\gamma\gamma \rightarrow \pi\pi; W_{\gamma\gamma}) S_{abs}^2(\mathbf{b}) \times N(\omega_1, \mathbf{b}_1) N(\omega_2, \mathbf{b}_2) \frac{W_{\gamma\gamma}}{2} d^2\mathbf{b}_1 d^2\mathbf{b}_2 dW_{\gamma\gamma} dY_{\pi\pi} \quad (4)$$

In the above approach one can easily calculate only the total nuclear cross section, distributions in rapidity of the pair of pions, and the invariant mass of the dipions (see e.g. [9, 3]), experimental constraints can not be easily imposed.

If one wants to calculate kinematical distributions of each of the individual particles (transverse momentum, rapidity, pseudorapidity), or impose corresponding experimental cuts, a more complicated calculation is required. Then instead of the one-dimensional function $\sigma(\gamma\gamma \rightarrow \pi\pi; W_i)$, a two-dimensional functions $\frac{d\sigma(\gamma\gamma \rightarrow \pi\pi)}{dz}(W_i, z_j)$ have to be calculated. Then an extra integration in $z = \cos\theta$ is required in Eqs. (1) or (4), which makes the calculation time-consuming.

Four-momenta of pions in the $\pi\pi$ center of mass frame can be calculated as:

$$E_\pi = \sqrt{\hat{s}}/2. ,$$

$$\begin{aligned}
p_\pi &= \sqrt{\frac{\hat{s}}{4} - m_\pi^2} , \\
p_{t,\pi} &= \sqrt{1 - z^2} p_\pi , \\
p_l &= z p_\pi .
\end{aligned} \tag{5}$$

The rapidity of the pion can be calculated as:

$$y_i = Y_{\pi\pi} + y_{i/\pi\pi} , \tag{6}$$

where $y_{i/\pi\pi} = y_{i/\pi\pi}(W, z)$ is the rapidity of one of the pions in the recoil $\pi\pi$ system. The transverse momenta of pions in both frames of reference are the same. Other kinematical variables are calculated by adding relativistically velocities [16]

$$\vec{v}_i = \vec{V}_{\pi\pi} \oplus \vec{v}_{i/\pi\pi} , \tag{7}$$

where

$$\vec{V}_{\pi\pi} = \frac{\vec{P}_{\pi\pi}}{E_{\pi\pi}} \tag{8}$$

and from the energy-momentum conservation:

$$\begin{aligned}
E_{\pi\pi} &= \omega_1 + \omega_2 , \\
P_{\pi\pi}^z &= \omega_1 - \omega_2 ,
\end{aligned} \tag{9}$$

the energies of photons can be expressed as:

$$\begin{aligned}
\omega_1 &= \frac{W_{\gamma\gamma}}{2} \exp(Y) , \\
\omega_2 &= \frac{W_{\gamma\gamma}}{2} \exp(-Y) .
\end{aligned} \tag{10}$$

Now the pion velocities can be converted to four-momenta of pions in the nucleus-nucleus center of mass frame. Then angles or pseudorapidities of pions can be calculated and experimental cuts can be imposed.

2.3. Single scattering production of ρ^0

Most of the analyses in the literature concentrated on production of pairs of mesons in photon-photon processes (see Fig. 2). Our group has studied both exclusive $\rho^0\rho^0$ productions [9] and recently exclusive production of $J/\psi J/\psi$ pairs.

In the case of double ρ^0 production there are two mechanisms. At larger photon-photon energies the pomeron/reggeon exchange mechanism is the dominant one, while close to $\rho^0\rho^0$ threshold a large enhancement was observed. In Ref. [9] this enhancement of the cross section was parametrized.

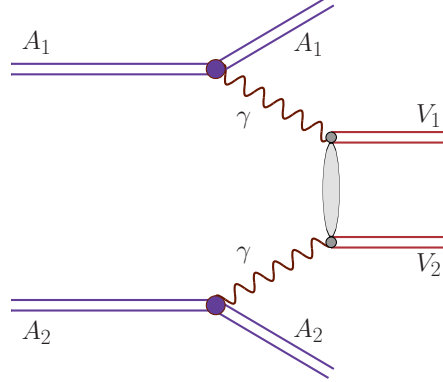


Fig. 2. (Color online) The photon-photon mechanism of two vector meson production in ultrarelativistic ultraperipheral collisions.

In the present paper we shall concentrate rather on larger dimeson invariant masses.

The elementary cross section for $\gamma\gamma \rightarrow \rho^0\rho^0$ has been measured in the past for not too large energies. The measured cross section shows a characteristic bump at about $M_{\rho\rho} \sim 1.5$ GeV.

At somewhat larger photon-photon energies (larger $\rho^0\rho^0$ invariant masses) another mechanism, which can be relatively reasonably calculated, plays the dominant role. This is a soft (small angle) virtual vector meson rescattering. The corresponding matrix element for small ρ^0 meson transverse momenta can be parametrized in the VDM-Regge approach [9]. At large transverse momenta of the ρ^0 meson, two-gluon exchange should become important. In the present analysis we shall discuss only the soft scattering mechanisms. The hard mechanism may be important at the LHC.

The nuclear cross section for the photon-photon mechanism is calculated in the impact parameter space as:

$$\sigma(AA \rightarrow AA\rho^0\rho^0) = \int \hat{\sigma}(\gamma\gamma \rightarrow \rho^0\rho^0; W_{\gamma\gamma}) S_{abs}^2(\mathbf{b}) N(\omega_1, \mathbf{b}_1) N(\omega_2, \mathbf{b}_2) \times d^2\mathbf{b}_1 d^2\mathbf{b}_2 d\omega_1 d\omega_2. \quad (11)$$

Above $W_{\gamma\gamma}$ is the energy in the $\gamma\gamma$ system and the factor related to absorption is taken as:

$$S_{abs}^2(\mathbf{b}) = \theta(\mathbf{b} - 2R_A) = \theta(|\mathbf{b}_1 - \mathbf{b}_2| - 2R_A). \quad (12)$$

This can be written equivalently as:

$$\sigma(AA \rightarrow AA\rho^0\rho^0) = \int \hat{\sigma}(\gamma\gamma \rightarrow \rho^0\rho^0; W_{\gamma\gamma}) S_{abs}^2(\mathbf{b}) N(\omega_1, \mathbf{b}_1) N(\omega_2, \mathbf{b}_2)$$

$$\times \frac{W_{\gamma\gamma}}{2} d^2 \mathbf{b}_1 d^2 \mathbf{b}_2 dW_{\gamma\gamma} dY_{\rho^0 \rho^0} . \quad (13)$$

Four-momenta of ρ^0 mesons in the $\rho^0 \rho^0$ center of mass frame read:

$$E_{\rho^0} = \frac{\sqrt{\hat{s}}}{2} , \quad (14)$$

$$p_{\rho^0} = \sqrt{\frac{\hat{s}}{4} - m_{\rho^0}^2} , \quad (15)$$

$$p_{t,\rho^0} = \sqrt{1 - z^2} p_{\rho^0} , \quad (16)$$

$$p_{l,\rho^0} = z p_{\rho^0} . \quad (17)$$

Above $\hat{s} = W_{\gamma\gamma}^2$ and $z = \cos \theta^*$ is defined in the $\rho^0 \rho^0$ center of mass frame. In calculations of the photon-photon processes the masses of ρ^0 mesons are set at their resonance values.

The rapidity of each of the ρ^0 mesons ($i = 1, 2$) is calculated as:

$$y_i = Y_{\rho^0 \rho^0} + y_{i/\rho^0 \rho^0}(W_{\gamma\gamma}, z) , \quad (18)$$

where z can be calculated using ρ^0 transverse momentum. $Y_{\rho^0 \rho^0}$ is rapidity of the $\rho^0 \rho^0$ system.

Other kinematical variables are calculated by adding relativistically velocities:

$$\vec{v}_i = \vec{v}_{\rho^0 \rho^0} \oplus \vec{v}_{i/\rho^0 \rho^0} , \quad (19)$$

$$\vec{v}_{\rho^0 \rho^0} = \frac{\vec{P}_{\rho^0 \rho^0}}{E_{\rho^0 \rho^0}} , \quad (20)$$

where $\vec{v}_{\rho^0 \rho^0}$ is velocity of the $\rho^0 \rho^0$ system in the overall nucleus-nucleus center of mass and $\vec{v}_{i/\rho^0 \rho^0}$ is velocity of one of the ρ^0 mesons in the $\rho^0 \rho^0$ system. $\vec{P}_{\rho^0 \rho^0}$ and $E_{\rho^0 \rho^0}$ are momentum and energy of the $\rho^0 \rho^0$ system.

The energies of photons is expressed in terms of our integration variables

$$\omega_{1/2} = \frac{W_{\gamma\gamma}}{2} \exp(\pm Y_{\rho^0 \rho^0}) \quad (21)$$

from the energy-momentum conservation:

$$\begin{aligned} E_{\rho^0 \rho^0} &= \omega_1 + \omega_2 , \\ P_{\rho^0 \rho^0}^z &= \omega_1 - \omega_2 . \end{aligned} \quad (22)$$

The total elementary cross section is calculated as:

$$\hat{\sigma}(\gamma\gamma \rightarrow \rho^0 \rho^0) = \int_{t_{min}(\hat{s})}^{t_{max}(\hat{s})} \frac{d\hat{\sigma}}{d\hat{t}} d\hat{t}, \quad (23)$$

where

$$\frac{d\hat{\sigma}(\gamma\gamma \rightarrow \rho^0 \rho^0)}{d\hat{t}} = \frac{1}{16\pi\hat{s}^2} |\mathcal{M}_{\gamma\gamma \rightarrow \rho^0 \rho^0}|^2. \quad (24)$$

The matrix element is calculated in a VDM-Regge approach [9] as

$$\begin{aligned} \mathcal{M}_{\gamma\gamma \rightarrow \rho^0 \rho^0} &= C_{\gamma \rightarrow \rho^0} C_{\gamma \rightarrow \rho^0} \hat{s} \left(\eta_{\mathbf{IP}}(\hat{s}, \hat{t}) C_{\mathbf{IP}} \left(\frac{\hat{s}}{s_0} \right)^{\alpha_{\mathbf{IP}}(t)-1} + \eta_R(\hat{s}, \hat{t}) C_R \left(\frac{\hat{s}}{s_0} \right)^{\alpha_R(t)-1} \right) \\ &\times F(\hat{t}, q_1^2 \approx 0) F(\hat{t}, q_2^2 \approx 0). \end{aligned} \quad (25)$$

This is consistent with the existing world experimental data on total $\gamma\gamma \rightarrow \rho^0 \rho^0$ cross section [9]. The photon-to- ρ^0 transformation $C_{\gamma \rightarrow \rho^0}$ factor is calculated in the Vector Dominance Model (VDM). The parameters responsible for energy dependence are taken from the Donnachie-Landshoff parametrization of the total proton-proton and pion-proton cross sections [17] assuming Regge factorization. The slope parameter is taken as $B = 4 \text{ GeV}^{-2}$. The form factors $F(\hat{t}, q^2)$ is described in detail in Ref. [9]. When calculating kinematical variables, a fixed resonance position $m_\rho = m_R$ is taken for the $\gamma\gamma \rightarrow \rho^0 \rho^0$.

The differential distributions can be obtained by replacing total elementary cross section by

$$\hat{\sigma}(\gamma\gamma \rightarrow \rho^0 \rho^0) = \int \frac{d\hat{\sigma}(\gamma\gamma \rightarrow \rho^0 \rho^0)}{dp_t} dp_t, \quad (26)$$

where

$$\frac{d\hat{\sigma}}{dp_t} = \frac{d\hat{\sigma}}{dp_t^2} \frac{dp_t^2}{dp_t} = \frac{d\hat{\sigma}}{dp_t^2} 2p_t = \frac{d\hat{\sigma}}{d\hat{t}} |\partial\hat{t}/\partial p_t^2| 2p_t. \quad (27)$$

The first ρ^0 is emitted in the forward and the second ρ^0 in the backward direction. The following three-dimensional grids are prepared separately for the low-energy bump and VDM-Regge components:

$$\frac{d\sigma_{AA \rightarrow AA \rho^0 \rho^0}}{dy_1 dy_2 dp_t}. \quad (28)$$

The grids are used then to calculate distributions of pions from the decays of ρ^0 mesons produced in the photon-photon fusion.

2.4. Single ρ^0 production

The cross section for single vector meson production, differential in impact factor and vector-meson rapidity, reads:

$$\frac{d\sigma}{d^2b dy} = \omega_1 \frac{d\tilde{N}}{d^2b d\omega_1} \sigma_{\gamma A_2 \rightarrow V A_2}(W_{\gamma A_2}) + \omega_2 \frac{d\tilde{N}}{d^2b d\omega_2} \sigma_{\gamma A_1 \rightarrow V A_1}(W_{\gamma A_1}) , \quad (29)$$

where $\omega_1 = m_{\rho^0}/2 \exp(+y)$ and $\omega_2 = m_{\rho^0}/2 \exp(-y)$. The flux factor of equivalent photons, \tilde{N} , is in principle a function of AA impact parameter b and not of photon-nucleus impact parameter as is usually done in the literature. The effective impact factor can be formally written as the convolution of real photon flux in one of the nuclei and effective strength for interaction of the photon with the second nucleus

$$\frac{d\tilde{N}}{d^2b d\omega} = \int \frac{dN}{d^2b_1 d\omega} \frac{S(b_2)}{\pi R_A^2} d^2b_1 \approx \frac{dN}{d^2b d\omega} , \quad (30)$$

where $\vec{b}_1 = \vec{b} + \vec{b}_2$ and $S(b_2) = \theta(R_A - b_2)$. It is assumed that the collision occurs when the photon hits the nucleus. For the photon flux in the second nucleus one needs to replace $1 \rightarrow 2$ and $2 \rightarrow 1$.

In general case one can write:

$$\sigma_{\gamma A \rightarrow V A}(W) = \frac{d\sigma_{\gamma A \rightarrow V A}(W, t=0)}{dt} \int_{-\infty}^{t_{max}} dt |F_A(t)|^2 . \quad (31)$$

Above W is energy in the γA system. The second factor includes the t -dependence for the $\gamma A \rightarrow V A$ subprocess which is due to coherent $q\bar{q}$ dipole rescattering off a “target” nucleus. This is dictated by the nuclear strong form factor. We approximate the nuclear strong form factor by the nuclear charge form factor. The t_{max} is calculated as $t_{max} = -(m_{\rho^0}^2/(2\omega_{lab}))^2$. $F_A(t)$ is calculated as Fourier transform of the Woods-Saxon charge distribution with parameters specified in Ref. [18]. The first term in Eq. (31) is usually weakly dependent on the γA energy. For the ρ^0 meson it is almost a constant [8]:

$$\frac{d\sigma(\gamma + A \rightarrow \rho^0 A; W, t=0)}{dt} \approx \text{const} . \quad (32)$$

The constant is taken to be (see [8]) 420 mb/GeV² for RHIC and 450 mb/GeV² for LHC. These are cross sections for $W_{\gamma p}$ energies relevant for midrapidities at $\sqrt{s_{NN}} = 200$ GeV and 5.5 TeV, respectively.

The second term in Eq.(31) depends on t_{max} which in turn depends rather on running ρ^0 meson mass than on resonance position.

The cross section for the $\gamma A \rightarrow VA$ reaction could be also calculated e.g., in the QCD dipole picture in the so-called mixed representation (see e.g., [20, 21]). For a more complicated momentum space formulation of the vector meson production on nuclei see [22].

At high energy the imaginary part of the amplitude for the $\gamma A \rightarrow VA$ process can be expressed as [23, 24]:

$$\Im(A_{\gamma A \rightarrow VA}(W)) = \Sigma_{\lambda\bar{\lambda}} \int dz d^2\rho \Psi_{\lambda\bar{\lambda}}^V(z, \rho) \sigma_{dip-A}(\rho, W) \Psi_{\lambda\bar{\lambda}}^\gamma(z, \rho). \quad (33)$$

In the equation above, λ and $\bar{\lambda}$ are quark and antiquark helicities. Helicity conservation at high energy rescattering of the dipole in the nucleus is assumed. The variable ρ is the transverse size of the quark-antiquark dipole, and $z/(1-z)$ denote the longitudinal momentum fractions carried by quark and antiquark, respectively. Using explicit formulae for photon and vector meson wave functions, the generic formula (33) can be written in a simple way. The dipole-nucleus cross section can be expressed in the Glauber-Gribov approach in terms of the nuclear thickness $T_A(b_\gamma)$, as seen by the $q\bar{q}$ dipole in its way through the nucleus, and the dipole-proton $\sigma_{dip-p}(\rho)$ cross section as:

$$\sigma_{dip-A}(\rho, W) = 2 \int d^2b_\gamma \left\{ 1 - \exp\left(-\frac{1}{2}T_A(b_\gamma)\sigma_{dip-p}(\rho, W)\right) \right\}. \quad (34)$$

The formula above allows for an easy way to include rather complex multiple scattering of the quark-antiquark dipole in the nucleus. Several parametrizations of the dipole-nucleon cross section were proposed in the literature. Most of them were obtained through fitting HERA deep-inelastic scattering data. The saturation inspired parametrizations are the most popular ones.

Before we go to double ρ^0 production, we briefly show the results for single ρ^0 production. In Fig. 3 we present distributions in rapidity. We obtain similar results as in other calculations in the literature [8, 19, 11]. We show rapidity distribution with $\frac{d\sigma(\gamma A \rightarrow \rho^0 A; t=0)}{dt} = 420 \text{ mb/GeV}^2$ and result obtained with the Glauber-VDM approach of Ref. [8] where the elementary cross section was parametrized in a Regge form with constant (energy-independent) slope. However, the change turned out to be rather small as it is shown in Fig.3.

It is sufficient for our double-scattering studies that our model describes single ρ^0 production in the measured region of midrapidities. We leave potential uncertainties related to larger rapidities for future studies. Our total cross section equals 596 mb. The results of models presented in [19] and [11] exceed the STAR experimental data [12].

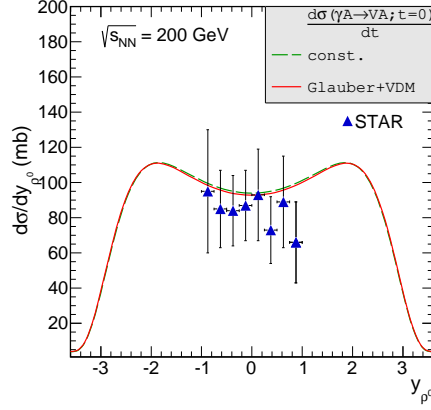


Fig. 3. (Color online) Distribution in ρ^0 rapidity for single ρ^0 . The STAR experimental data are from Ref. [12]. The dashed line is for $d\sigma/dt = \text{const}$ and the solid line is for $d\sigma/dt$ calculated in the Glauber-VDM approach.

2.5. Double scattering mechanism of two ρ^0 production

The generic diagrams of double-scattering production via photon-pomeron or pomeron-photon exchange¹ mechanism are shown in Fig. 4.

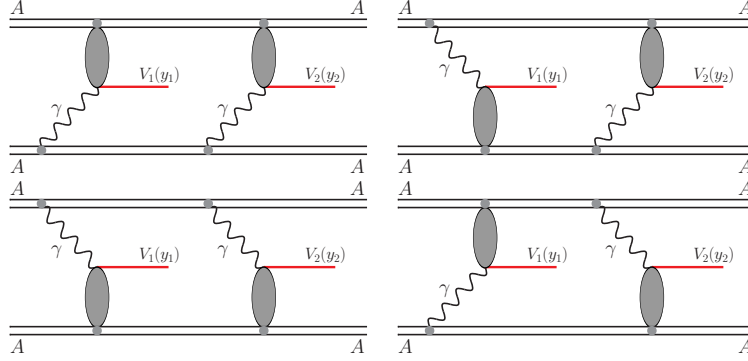


Fig. 4. (Color online) The double-scattering mechanisms of two vector meson production. The blobs denote multiple scattering of quark-antiquark dipoles or hadronic meson-like photon in the nucleus.

¹ For brevity and by analogy to nucleon-nucleon collisions we use the term “pomeron exchange” which in fact means complicated high-energy multiple diffractive rescattering of quark-antiquark pairs or virtual vector mesons.

The double scattering process was discussed only in Ref. [8], where a probabilistic formula for double and multiple vector meson production was given. Then the cross section for double scattering can be written as:

$$\sigma_{AA \rightarrow AAV_1 V_2}(\sqrt{s_{NN}}) = C \int S_{el}^2(b) P_{V_1}(b, \sqrt{s_{NN}}) P_{V_2}(b, \sqrt{s_{NN}}) d^2b . \quad (35)$$

In the equation above b is the transverse distance between nuclei. We have included natural limitations in the impact parameter

$$S_{el}^2(b) = \exp\left(-\sigma_{NN}^{tot} T_{A_1 A_2}(b)\right) \approx \theta(b - (R_1 + R_2)) . \quad (36)$$

This may be interpreted as a survival probability for nuclei not to break up. The probability density of single vector meson production is

$$P_V(b, \sqrt{s_{NN}}) = \frac{d\sigma_{AA \rightarrow AAV}(b; \sqrt{s_{NN}})}{2\pi b db} . \quad (37)$$

The constant C is in the most general case 1 or $\frac{1}{2}$ for identical vector mesons $V_1 = V_2$. We have explicitly indicated the dependence of the probabilities on nucleon-nucleon energy. The probability densities P_V increase with increasing cm energy.

Here the photon flux factor is calculated as:

$$\frac{d^3 N}{d^2 b d\omega} = \frac{Z^2 \alpha_{em} X^2}{\pi^2 \omega b^2} K_1^2(X) , \quad (38)$$

where $X = \frac{b\omega}{\gamma}$.

The simple formula (35) can be generalized to calculate two-dimensional distributions in rapidities of both vector mesons

$$\begin{aligned} \frac{d\sigma_{AA \rightarrow AAV_1 V_2}}{dy_1 dy_2} = C \int & \left(\frac{dP_1^{\gamma \mathbf{P}}(b, y_1; \sqrt{s_{NN}})}{dy_1} + \frac{dP_1^{\mathbf{P} \gamma}(b, y_1; \sqrt{s_{NN}})}{dy_1} \right) \\ & \times \left(\frac{dP_2^{\gamma \mathbf{P}}(b, y_2; \sqrt{s_{NN}})}{dy_2} + \frac{dP_2^{\mathbf{P} \gamma}(b, y_2; \sqrt{s_{NN}})}{dy_2} \right) d^2b \end{aligned} \quad (39)$$

P_1 and P_2 are probability densities for producing one vector meson V_1 at rapidity y_1 and the second vector meson V_2 at rapidity y_2 for the impact parameter b . Then the differential probability density reads:

$$\frac{dP_V(b, \sqrt{s_{NN}})}{dy} = \frac{d\sigma_{AA \rightarrow AAV}(b; \sqrt{s_{NN}})}{2\pi b db dy} . \quad (40)$$

The produced vector mesons in each step are produced in very broad range of (pseudo)rapidity [8, 20] and extremely small transverse momenta.

3. Results

3.1. $PbPb \rightarrow PbPb\pi\pi$

We start presentation of our results in Fig.5 by showing interesting distribution in impact parameter between the two lead nuclei. The distribution is different from zero starting from the distance of $b = 2R_A \approx 14$ fm and extends till "infinity". This means that a big part of the cross section comes from the situations when the two ^{208}Pb nuclei fly far one from the other. This demonstrates the ultraperipheral character of the discussed process of exclusive dipion production via photon-photon fusion.

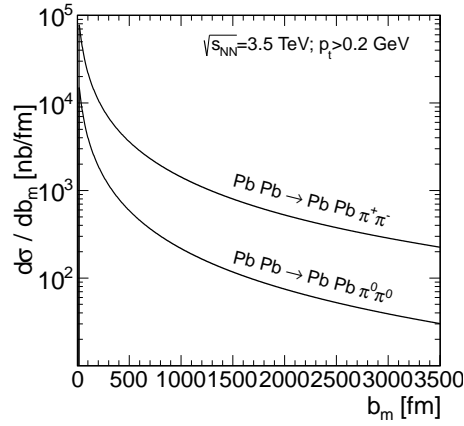


Fig.5. (Color online) The impact parameter distribution for the $PbPb \rightarrow PbPb\pi^+\pi^-$ and $PbPb \rightarrow PbPb\pi^0\pi^0$ reactions at $\sqrt{s_{NN}} = 3.5$ TeV.

The distribution in invariant dipion mass is shown in Fig.6. The distribution for the full phase space (upper solid line) is shown for the $PbPb \rightarrow PbPb\pi^+\pi^-$ (left panel) and for the $PbPb \rightarrow PbPb\pi^0\pi^0$ (right panel) reactions for the full phase space (upper lines), for $|\cos\theta| < 0.9$ (middle lines) and for $|\cos\theta| < 0.8$ (lowest line). At lower dipion invariant masses the result does not depend on the angular cuts.

Let us start now presentation of theoretical differential distributions that can be measured. In the left panel of Fig.7 we show distributions in rapidity of individual pions (solid line) and distribution in pseudorapidity of the same pion (dashed line). Right panel illustrates nuclear cross section as the function of the pion pair rapidities. Here we have imposed extra cuts on pion transverse momenta: $p_{t,\pi} > 0.2$ GeV (solid lines) and $p_{t,\pi} > 0.5$ GeV (dashed lines). In addition, we compare the nuclear cross section for $\pi^+\pi^-$ (upper curves) and for $\pi^0\pi^0$ (lower curves) production.

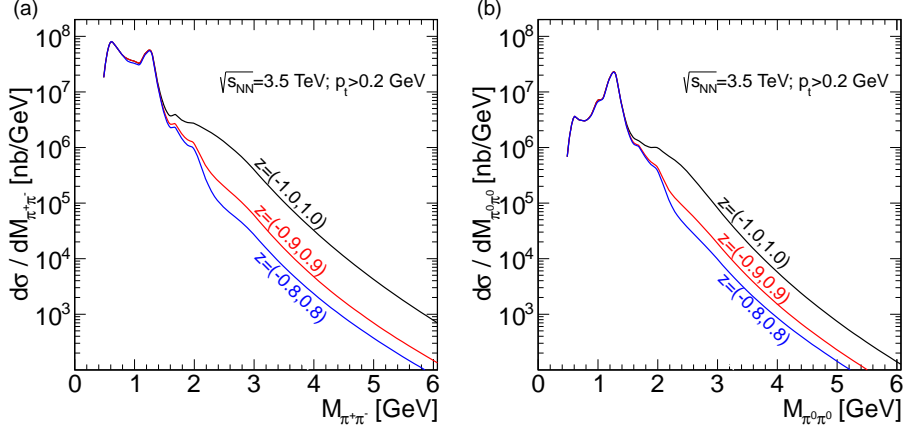


Fig. 6. (Color online) Dipion invariant mass for $\pi^+\pi^-$ (left panel) and $\pi^0\pi^0$ (right panel) at the LHC energy $\sqrt{s_{NN}} = 3.5$ TeV and $p_{t,\pi} > 0.2$ GeV. We show also results with extra cuts on z .

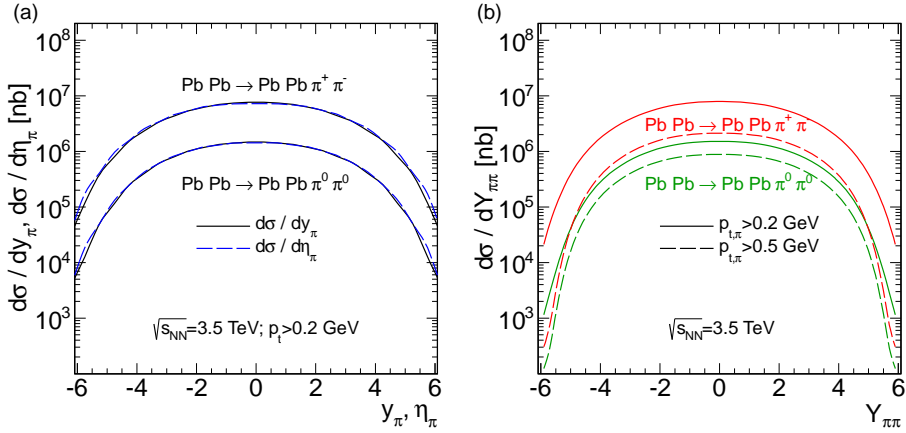


Fig. 7. (Color online) $\frac{d\sigma}{dy_{\pi}}$ and $\frac{d\sigma}{d\eta_{\pi}}$ (left panel) and $\frac{d\sigma}{dY_{\pi\pi}}$ (right panel) for the LHC energy $\sqrt{s_{NN}} = 3.5$ TeV.

In Fig.8 the resonance contribution for the $\rho^0(1450)$ is 5/0.27 times smaller than for $\rho^0(770)$ as suggested by a calculation in the literature and the above upper limit for the branching fraction into pions. It is clear that this is an upper estimate for the $\rho^0(1450)$ contribution.

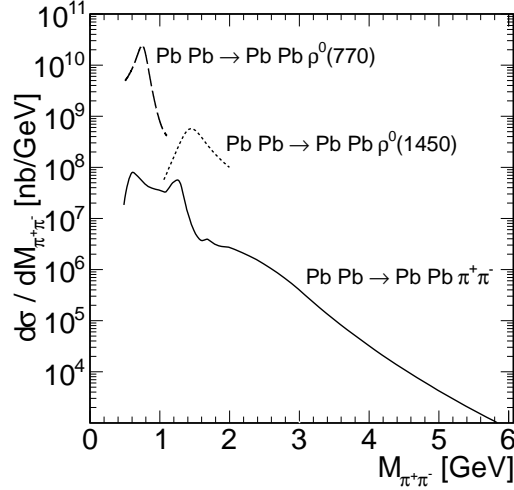


Fig. 8. Invariant mass distribution of $\pi^+\pi^-$ from the decay of $\rho^0(770)$ and $\rho^0(1450)$ photo-production (resonance contributions represented by the dashed and dotted lines) and our $\gamma\gamma$ fusion (solid line) in ultraperipheral Pb-Pb collisions at $\sqrt{s_{NN}} = 3.5$ TeV.

3.2. Exclusive production of $\rho^0\rho^0$ pairs

Now we shall discuss production of $\rho^0\rho^0$ pairs.

Distributions in ρ^0 meson rapidity is shown in Fig. 9. One observes a dominance of the double scattering component over the photon-photon component. At the LHC the proportions will be slightly modified. For the photon-photon mechanism we show separate contributions for the forward and backward ρ^0 mesons.

The corresponding distribution in the $\rho^0\rho^0$ invariant mass is shown in Fig. 10. We show both low-energy and high-energy photon-photon contributions. The low energy component is a purely mathematical fit from Ref.[9]. This may be a bit an artifact of a simple functional form used. The issue is a bit difficult as the peak appears close to the threshold. This could be also some close to threshold mechanism. Our purely mathematical representation of the unknown effect is therefore oversimplified. In general, larger invariant masses are generated via the double scattering mechanism than in two-photon processes. The reader is asked to compare the present plot with analogous plot in Ref. [9].

In experiments, charged pions are measured rather than ρ^0 mesons. Therefore, we now proceed to a presentation of some observables related to charged pions. In Fig. 11 we present four-pion invariant mass distribu-

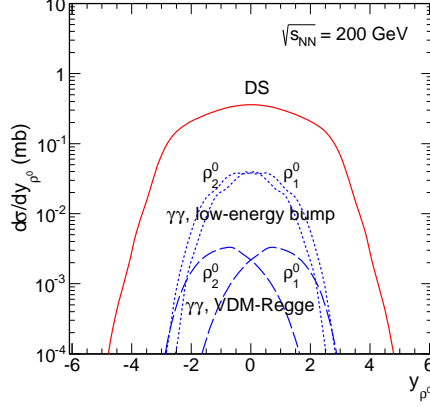


Fig. 9. (Color online) Rapidity distribution of one of ρ^0 mesons produced in double scattering mechanism. The double-scattering contribution is shown by the solid (red online) line and the dashed lines (blue online) represents distributions of ρ^0 produced in the high-energy VDM-Regge photon-photon fusion.

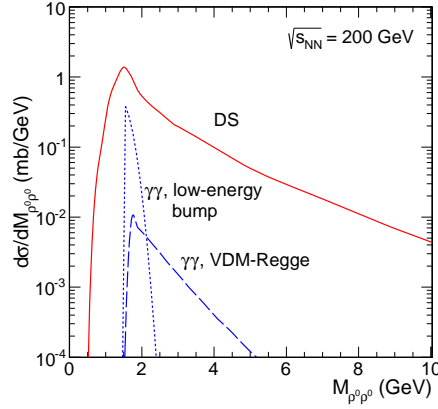


Fig. 10. (Color online) Invariant mass distribution of $\rho^0\rho^0$ for double scattering (solid line), high-energy VDM-Regge photon-photon (dashed line) and low-energy bump (dotted line) contributions for full phase space.

tion. The distribution for the whole phase space extends to large invariant masses, while the distribution in the limited range of (pseudo)rapidity as defined by the STAR detector give a shape similar to the measured distribution (see dash-dotted line in the right panel of Fig. 11). However, the

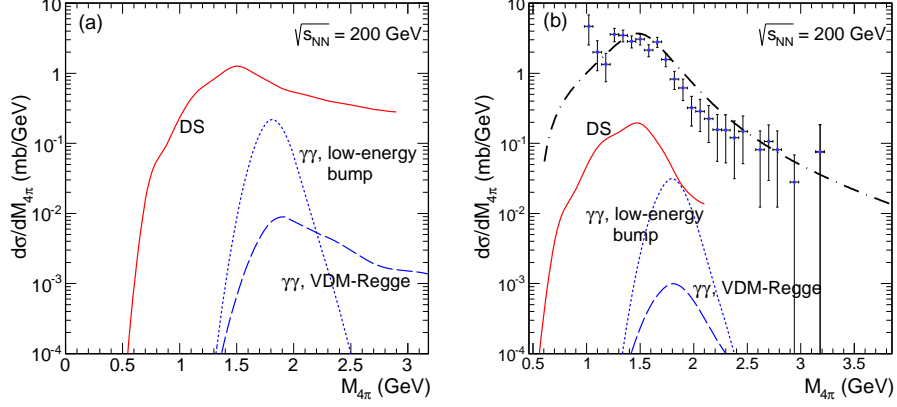


Fig. 11. (Color online) Four-pion invariant mass distribution for double scattering mechanism (solid line), high-energy VDM-Regge photon-photon (dashed line) and low-energy bump (dotted line) mechanisms for full phase space (left panel) and for the limited acceptance STAR experiment (right panel). The STAR experimental data [25] have been corrected by acceptance function [26]. The dash-dotted line represents a fit of the STAR collaboration.

double-scattering contribution accounts only for 20 % of the cross section measured by the STAR collaboration [25]. Probably, the production of the $\rho^0(1700)$ resonance and its subsequent decay into the four-pion final state (see e.g., [27]) is the dominant effect for the limited STAR acceptance. Both, the production mechanism of $\rho^0(1700)$ and its decay into four charged pions are not yet fully understood. There was only one attempt to calculate the production cross section in the Glauber-Gribov GVDM approach [28]. Furthermore there is another broad $\rho(1450)$ resonance [27] which also decays into four charged pions. We leave the modeling of the production and decay processes for a dedicated study.

In Fig. 12 we show distributions in pseudorapidity of the charged pions. The distributions extend over a broad range of pseudorapidity. Both STAR collaboration at RHIC and the ALICE collaboration at LHC can observe only a small fraction of pions due to the rather limited pseudorapidity coverage. While the CMS pseudorapidity coverage is wider, it is not clear if the CMS collaboration has a relevant trigger to measure the exclusive nuclear processes.

For completeness in Fig. 13 we show distributions in pion transverse momenta. Since the ρ^0 mesons produced in the double-scattering photon-induced mechanisms have very small transverse momenta, the transverse

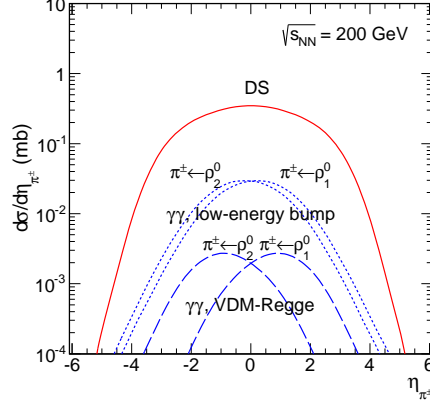


Fig. 12. (Color online) Pseudorapidity distribution of charged pions for double scattering (solid line), high-energy VDM-Regge photon-photon (dashed line) and low-energy bump (dotted line) mechanisms for full phase space.

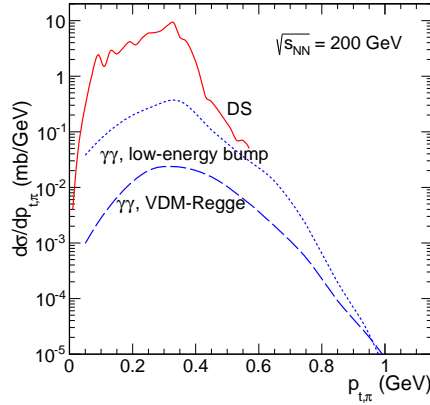


Fig. 13. (Color online) Transverse momentum distribution of charged pions for double scattering (solid line) low-energy bump (dotted line) and high-energy VDM-Regge photon-photon (dashed line) mechanisms for full phase space.

momenta of pions are limited to $\sim m_{\rho^0}/2$. The distribution is relatively smooth, because here we have taken into account a smearing of ρ^0 meson masses. The sharp upper limit is an artifact of our maximal value of ρ^0 meson mass $m_{\rho}^{max} = 1.2$ GeV. We have imposed this upper limit because the spectral shape of “ ρ^0 meson” above $m_{\rho} > 1.2$ GeV is not well known.

At larger $p_{t,\pi}$, the contribution from the decay of ρ^0 meson produced in photon-photon fusion can be larger as that of double scattering mechanism, as the transverse momentum of ρ^0 mesons are not strictly limited to small values. However, the cross section for such cases is expected to be very small. Both STAR ($p_t > 0.1$ GeV) and ALICE ($p_t > 0.1$ GeV) experiments have a fairly good coverage in pion transverse momenta and could measure such distributions.

4. Conclusions

In Ref.[15] we have calculated total cross sections and angular distribution as a function of $\gamma\gamma$ energy for both $\gamma\gamma \rightarrow \pi^+\pi^-$ and $\gamma\gamma \rightarrow \pi^0\pi^0$ processes. These energy-dependent cross sections have been used in Equivalent Photon Approximation in the impact parameter space to calculate corresponding production rate in ultraperipheral ultrarelativistic heavy ion reactions. In this calculation we have taken into account realistic charge distributions in colliding nuclei.

We have calculated both total cross sections at LHC energy, and distributions in rapidity and transverse momentum of pions and dipion invariant mass. The calculation of distributions of individual pions in the b-space EPA is more complicated. The distributions in dipion invariant mass have been compared with the contribution of exclusive $\rho^0 \rightarrow \pi^+\pi^-$ production in photon-pomeron or pomeron-photon mechanism. Close to the ρ^0 resonance the $\gamma\gamma \rightarrow \pi^+\pi^-$ mechanism yields only a small contribution. We hope the $\gamma\gamma$ contribution could be identified or even measured outside of the ρ^0 resonance region. A detailed comparison with the absolutely normalized experimental data of the ALICE collaboration should allow a test of our predictions. We have discussed two- ρ^0 as well as four-pion production in exclusive ultraperipheral heavy ion collisions, concentrating on the double scattering mechanism.

Differential distributions for the two ρ^0 mesons and for four pions have been presented. The results for total cross section and differential distributions for the double scattering mechanism have been compared with the results for two-photon fusion discussed already in the literature. We have found that at $\sqrt{s_{NN}} = 200$ GeV the contribution of double scattering is almost two orders of magnitude larger than that for the photon-photon mechanism.

The produced ρ^0 mesons decay, with large probability, into charged pions. In the consequence this leads to large contribution to exclusive production of the $\pi^+\pi^-\pi^+\pi^-$ final state. We have made a comparison of four pion production via $\rho^0\rho^0$ production (double scattering and photon-photon fusion) with experimental data measured by the STAR collaboration for

gold-gold scattering. The theoretical predictions have fairly similar shape in four-pion invariant mass distribution as measured by the STAR collaboration but exhaust only a quarter of the measured cross section. The missing contribution is probably due to the exclusive production of $\rho^0(1700)$ resonance and its decay into four charged pions. We expect that in the total phase space the contribution of double scattering is similar to that for the $\rho^0(1700)$ resonant production.

A separation of double scattering, photon-photon and ρ' mechanisms seems very important. In general, transverse momentum of each of the produced ρ^0 's in double scattering mechanism is very small, smaller than in the other mechanisms. As a consequence the pions from the decay of ρ^0 's from the double-scattering mechanism are produced back-to-back in azimuthal angle. This could be used to enhance the signal of double scattering mechanism. At large pseudorapidity separations between two ρ^0 's and/or large $\pi^+\pi^+$ ($\pi^-\pi^-$) pseudorapidity separations the double scattering contribution should dominate over other contributions. The identification of the region seems difficult at RHIC but could be better at the LHC.

At present the four charged pion final state is being analyzed by the ALICE collaboration. We plan a separate careful analysis for the ALICE and other LHC experiments. It would be valuable if the different mechanisms discussed in the present paper could be separated experimentally in the future. This requires, however, rather complicated correlation studies for four charged pions.

Similar double scattering mechanisms could be studied for different vector meson production, e.g. for $\rho^0 J/\Psi$ production. Recently we have studied production of $J/\Psi J/\Psi$ pairs via two-photon mechanism [29]. A calculation of the corresponding double-scattering contribution would be in this case very interesting.

Acknowledgments

This presentation is based on common work with Mariola Khusek-Gawenda and Wolfgang Schäfer. This work was partially supported by N DEC-2011/01/B/ST2/04535.

REFERENCES

- [1] V.M. Budnev, I.F. Ginzburg, G.V. Meledin and V.G. Serbo, Phys. Rep. **15** (1975) 4; C.A. Bertulani and G. Baur, Phys. Rep. **163** (1988) 29; G. Baur, K. Hencken, D. Trautmann, S. Sadovsky, and Y. Kharlov, Phys. Rep. **364**

- (2002) 359; A.J. Baltz, G. Baur, D. d’Enterria et al., Phys. Rep. **458** (2008) 1.
- [2] R. Engel, A. Schiller and V.G. Serbo, Z. Phys. **C71** (1996) 651; U.D. Jentschura and V.G. Serbo, Eur. Phys. J. **C64** (2009) 309.
 - [3] M. Khusek-Gawenda and A. Szczurek, Phys. Rev. **C82** (2010) 014904.
 - [4] G. Baur and L. G. Ferreira Filho, Nucl. Phys. **A518** (1990) 786.
 - [5] J. Nystrand and S. Klein, arXiv:nucl-ex/9811007.
 - [6] V.P. Goncalves and M.V.T. Machado, Eur. Phys. J. **C29** (2003) 271.
 - [7] V.P. Goncalves, M.V.T. Machado and W.K. Sauter, Eur. Phys. J. **C46** (2006) 219.
 - [8] S.R. Klein and J. Nystrand, Phys. Rev. **C60** (1999) 014903.
 - [9] M. Khusek, A. Szczurek, and W. Schäfer, Phys. Lett. **B674** (2009) 92.
 - [10] L. Frankfurt, M. Strikman and M. Zhalov, Phys. Rev. **C67** (2003) 034901.
 - [11] V.P. Goncalves and M.V.T. Machado, Eur. Phys. J. **C40** (2005) 519; Phys. Rev. **C80** (2009) 054901.
 - [12] STAR Collaboration, B.I. Abelev et al., Phys. Rev. **C77** (2008) 034910.
 - [13] LHCb Collaboration, R. Aaij et al., J. High Energy Phys. **06** (2012) 141.
 - [14] M. Łuszczak, R. Maciula and A. Szczurek, Phys. Rev. **D84** (2011) 114018; R. Maciula and A. Szczurek, Phys. Rev. **D87** (2013) 074039.
 - [15] M. Khusek-Gawenda and A. Szczurek, Phys. Rev. **C87** (2013) 054908.
 - [16] R. Hagedorn, Relativistic Kinematics, High Energy Physics: W.A. Benjamin, Inc. Reading Massachusetts 1963.
 - [17] A. Donnachie and P.V. Landshoff, Phys. Lett. **B296** (1992) 227.
 - [18] M. Khusek-Gawenda and A. Szczurek, Phys. Rev. **C89** (2014) 024912.
 - [19] L. Frankfurt, M. Strikman and M. Zhalov, Phys. Rev. **C67** (2003) 034901.
 - [20] V.P. Goncalves and M.V.T. Machado, J. Phys. G. **32** (2006) 295.
 - [21] T. Lappi and H. Mäntysaari, Phys. Rev. **C87** (2013) 032201.
 - [22] A. Cisek, W. Schäfer and A. Szczurek, Phys. Rev. **C86** (2012) 014905.
 - [23] B.Z. Kopeliovich, J. Nemchik, N.N. Nikolaev and B.G. Zakharov, Phys. Lett. **B309** (1993) 179; Phys. Lett. **B324** (1994) 469.
 - [24] J. Nemchik, N.N. Nikolaev and B.G. Zakharov, Phys. Lett. **B341** (1994) 228; J. Nemchik, N.N. Nikolaev, E. Predazzi and B.G. Zakharov, Z. Phys. **C75** (1997) 71.
 - [25] STAR Collaboration, B.I. Abelev et al., Phys. Rev. **C81** (2010) 044901.
 - [26] Boris Grube, private communication.
 - [27] J. Beringer et al. (Particle Data Group), Phys. Rev. **D86** (2012) 010001.
 - [28] L. Frankfurt, M. Strikman and M. Zhalov, Acta Phys. Polon. **B34** (2003) 3215.
 - [29] S. Baranov, A. Cisek, M. Khusek-Gawenda, W. Schäfer and A. Szczurek, Eur. Phys. Jour. **C73** (2013) 2335.